



Status epilepticus induces a particular microglial activation state characterized by enhanced purinergic signaling.

Elena Avignone, Lauriane Ulmann, Françoise Levavasseur, François Rassendren, Etienne Audinat

► **To cite this version:**

Elena Avignone, Lauriane Ulmann, Françoise Levavasseur, François Rassendren, Etienne Audinat. Status epilepticus induces a particular microglial activation state characterized by enhanced purinergic signaling.: Activated microglia in the epileptic hippocampus. *Journal of Neuroscience*, Society for Neuroscience, 2008, 28 (37), pp.9133-44. <10.1523/JNEUROSCI.1820-08.2008>. <hal-00322326>

HAL Id: hal-00322326

<https://hal.archives-ouvertes.fr/hal-00322326>

Submitted on 17 Sep 2008

HAL is a multi-disciplinary open access archive for the deposit and dissemination of scientific research documents, whether they are published or not. The documents may come from teaching and research institutions in France or abroad, or from public or private research centers.

L'archive ouverte pluridisciplinaire **HAL**, est destinée au dépôt et à la diffusion de documents scientifiques de niveau recherche, publiés ou non, émanant des établissements d'enseignement et de recherche français ou étrangers, des laboratoires publics ou privés.

Section: Neurobiology of disease

Senior editor: Serge Przedborski

**Status epilepticus induces a specific microglial activation state
characterized by enhanced purinergic signaling**

Elena Avignone^{1,2,3}, Lauriane Ulmann⁴, Françoise Levavasseur^{1,2,3}, François Rassendren⁴,
Etienne Audinat^{1,2,3}

¹Inserm U603, Paris, France; ²CNRS UMR 8154, Paris, France; ³Université Paris Descartes, Paris, France. ⁴CNRS, UMR 5203, Institut de Génomique fonctionnelle, Montpellier, France; Inserm U661, Montpellier, France; Université Montpellier, 1,2, Montpellier, France.

Running title: Activated microglia in the epileptic hippocampus

Corresponding author: Etienne Audinat, Laboratoire de Neurophysiologie et Nouvelles Microscopies; INSERM U603, CNRS UMR 8154; Université Paris Descartes; 45, rue des Saints-Pères; 75006 Paris; FRANCE. Tel: 33-1-42864154; FAX: 33-1-42864151.

e-mail address: etienne.audinat@univ-paris5.fr

Manuscript information:

Figures:8; text pages: 28; words in the abstract: 240, introduction: 538, discussion: 1652.

Text pages in supplemental material: 0; figures in supplemental material: 2; Video in supplemental material: 2.

Keywords: Glial cells; ATP, inflammation, epilepsy, cytokines, hippocampus

Acknowledgements: We thank Mireille Lerner-Natoli and Fédérica Bertaso for helping with the *in vivo* recordings and for encouraging discussions. We thank David Julius for the gift of the P2Y12 antibody, Alexis Menteyne for some *in vitro* tests and Serge Charpak for critical comments on the manuscript. This work was funded by grants from Inserm (Avenir program), Agence Nationale de la Recherche (ANR), Fédération Française de la Recherche pour l'Epilepsie (FFRE) and Fondation Bettencourt-Schueller.

Abstract

Microglia cells are the resident macrophages of the central nervous system and their activation plays a critical role in inflammatory reactions associated with many brain disorders, including ischemia, Alzheimer and Parkinson's diseases and epilepsy. Yet, the changes of microglia functional properties in epilepsy have rarely been studied. Here, we used a model of status epilepticus (SE) induced by intra-peritoneal kainate injections to characterize the properties of microglial cells in hippocampal slices from CX3CR1^{eGFP/+} mice. SE induced within 3 hours an increased expression of inflammatory mediators in the hippocampus, followed by a modification of microglia morphology, a microglia proliferation and a significant neurodegeneration in CA1. Changes in electrophysiological intrinsic membrane properties of hippocampal microglia were detected at 24-48 hours post SE with, in particular, the appearance of new voltage-activated potassium currents. Consistent with the observation of an up-regulation of purinergic receptor mRNAs in the hippocampus, we also provide pharmacological evidence that microglia membrane currents mediated by the activation of P2 receptors, including P2X7, P2Y6 and P2Y12, were increased 48 hours after SE. As a functional consequence of this modification of purinergic signaling, motility of microglia processes toward a source of P2Y12 receptor agonist was twice faster in the epileptic hippocampus. This study is the first functional description of microglia activation in an *in vivo* model of inflammation and provides evidence for the existence of a specific microglial activation state after a status epilepticus.

Introduction

Increasing evidence indicates that inflammation is a landmark for a number of acute and chronic brain disorders including neuropathologies associated with seizures (Rock and Peterson, 2006;Choi and Koh, 2008). For instance, an increased expression of inflammatory markers has been observed in surgically resected temporal tissues from patients with temporal lobe epilepsy (Sheng et al., 1994;Crespel et al., 2002;Vezzani and Granata, 2005). A similar inflammatory reaction has also been reported in experimental models of temporal lobe epilepsy. In particular, an increase of pro-inflammatory cytokines and of markers of the innate immunity (IL-1 β , IL-6, TNF- α NF- κ B system, COX-2, prostaglandins, Toll-like receptors) has been detected in the rat hippocampus, starting within the first hour following the induction of a status epilepticus and lasting several days (Eriksson et al., 1999;De Simoni et al., 2000;Vezzani et al., 2008).

Microglia and astrocytes represent the major source of pro-inflammatory molecules and they play a critical role in determining the spatial and temporal extent of inflammation as well as its impact on neuronal function and survival (Wyss-Coray and Mucke, 2002;Hanisch and Kettenmann, 2007;Vesce et al., 2007;Viviani et al., 2007). Accordingly, microglia and astrocytes become reactive after a status epilepticus. In the case of microglia, this activation has been well documented in terms of changes in morphology and expression of specific markers (Vezzani and Granata, 2005). Yet, activation of microglial cells is a complex process that includes changes in pharmacological and electrophysiological properties, migration, proliferation and release of a variety of mediators (Farber and Kettenmann, 2005;Hanisch and Kettenmann, 2007). However, these functional properties have never been investigated in epileptic tissues. Furthermore, different stimuli and stimulatory contexts can trigger different activation states of microglial cells and the concept of a continuum of activation between quiescent and fully activated microglia has recently emerged (Hanisch and Kettenmann, 2007). Thus, the specific state of microglia after a status epilepticus cannot be inferred from our knowledge of other models.

Among the key signals that govern microglia activation, several lines of evidence indicate that ATP released by glia and neurons and acting through ionotropic (P2X) and metabotropic (P2Y) purinergic receptors regulates numerous aspects of microglia activation (Inoue et al., 2007). In particular, specific functions of different purinergic receptors in microglia have been identified pointing at essential roles of P2Y6 in phagocytosis (Koizumi et al., 2007), P2Y12 in the polarization, migration and process extension (Davalos et al., 2005;Haynes et al., 2006;Ohsawa et al., 2007) and P2X receptors in the secretion of pro-inflammatory molecules

from microglial cells (Tsuda et al., 2003; Coull et al., 2005; Chessell et al., 2005; Skaper et al., 2006). Interestingly, activation of microglia can differentially regulate the expression of its purinergic receptors in different models, as reported for P2X4, P2X7, P2Y6 and P2Y12 (Tsuda et al., 2003; Franke et al., 2004; Haynes et al., 2006; Koizumi et al., 2007; Kobayashi et al., 2008).

The aim of the present work was to characterize the activation state of hippocampal microglia during the inflammatory reaction which occurs in a non invasive model of status epilepticus (*i.e.* intra-peritoneal injection of kainate) in mice. We used CX3CR1^{eGFP/+} mice in which microglia expresses the green fluorescent protein and retains normal functional properties (Cardona et al., 2006), allowing the comparison of cellular characteristics between non-activated and activated microglia. Our data provide the first comprehensive functional characterization of activated microglia in the epileptic hippocampus.

Materials and Methods

Animals and seizure inductions

All experiments followed European Union and institutional guidelines for the care and use of laboratory animals (Council directive 86/609EEC). The heterozygous CX3CR1^{eGFP/+} mice used throughout this study were obtained by crossing CX3CR1^{eGFP/eGFP} (Jung et al., 2000) with C57BL/6 (Janvier, Le Genest Saint Isle, France) wild type mice. Intra-peritoneal (i.p.) injection of kainate (18-22 mg/kg) in phosphate buffer saline (PBS) was used to induce a status epilepticus in 30 to 40 day-old mice, while age matched PBS injected animals were used as control. Animals were observed and classified according to the Racine scale: 1) freezing behaviour; 2) rigid posture with straight and rigid tail; 3) repetitive head bobbing, rear into a sitting position with forepaws shaking; 4) rearing and falling, jumping, running with period of total stillness; 5) continuous level 4; 6) lost of posture and generalized convulsion activity, usually preceding death. After kainate injection, mice showed progression through the different stages, usually entering in phase 1 between 15 minutes after the injection and reaching stage 3 in 30-45 minutes. Animals not showing the normal progression were re-injected with half dose. Only animals reaching at least stage 4 were considered for this study. The duration of crises varied from 2 to 4 hours and mortality was around 20%.

Western blotting

The hippocampi of three mice per condition were homogenized in a lysis buffer (10mM HEPES buffer pH 7.4), 0.5% Triton X-100, and protease inhibitor cocktail (Roche Applied System). Lysates were clarified by centrifugation and protein concentration determined using protein assay kit (Biorad). Proteins were separated on reducing 12 % SDS– PAGE, and transferred on nitrocellulose membrane. The membrane was blocked with 5% non-fat dry milk/ 0.5% Tween 20 in Tris buffer saline (TBST) overnight at 4°C. The membrane was incubated overnight at 4°C with a rabbit anti-Iba1 (1/1000, Wako Chemicals GmbH, Neuss, Germany) in TBST and with mouse anti-tubuline (1:2500, Sigma-Aldrich, Lyon, France). After three washes in TBST, the membrane was then treated with HRP-conjugated secondary antibody for 1h at room temperature and revealed with ECL+ detection kit (Amersham).

Histochemistry

Mice were anesthetized with pentobarbital (50mg/kg) or Urethane (2g/Kg) and perfused transcardiacally with 4% paraformaldehyde in 0.1M phosphate buffer. Brains were dissected out, post-fixed for 2 hours or overnight at 4°C, and 50 µm thick slices were prepared with a VT 1000 Leica vibratome. Slices were washed 3 times with PBS and incubated for 2h with PBS containing 2 % Bovine Serum Albumine (Sigma-Aldrich, Lyon, France) and 0.1 % Triton X-100 (Sigma-Aldrich, Lyon, France). After 3 washes, slices were incubated overnight with primary antibodies for microglia markers Iba1 (rabbit polyclonal, 1/1000, Wako Chemicals GmbH, Neuss, Germany), MAC2 (1/1000, rat monoclonal, kindly provided by M. Benhamou, obtained from hybridomas (TIB-166) distributed by ATCC), P2Y12 (1/200, kindly provided by David Julius). Ki67 antibody (mice monoclonal, 1/20, BD Pharmigen) was used to assess cell proliferation. Appropriate secondary antibodies were applied for 2 hours at room temperature, included anti-rabbit/anti-rat IgG Alexa fluor 568/555 (1/1000, Invitrogen, Paisley, UK), anti-mouse IgG Alexa fluor 555 (1/1000, Chemicon). After staining, brain slices were mounted in Vectashield H1400 (Vector lab, distributed by Abcys, Paris France) and examined with a confocal laser-scanning microscope (Zeiss 510).

To assess neuronal damage, slices were incubated with eosin-hematoxylin solution for 10 seconds following by 5 washes with distilled water. For Fluorojade B staining, slices were successively immersed at room temperature in a solution of 5% NaOH in 80% ethanol for 5 min, 2 min in 70% ethanol, 2 min in distilled water, 10 min in 0.06% potassium permanganate, 2 min of distilled water. Slices were incubated for 20 min with 0.004% FluorojadeB in a 0.1% acetic acid and rinsed by 3 washes with distilled water. Slices were mounted and images of the hippocampal rostral region were captured with a Leica DMRA2

fluorescence microscope equipped with a 20x objective. To quantify FluorojadeB positive cells, three mice per condition (PBS or 48 hours after SE) were used. For each hippocampus, usually two fields (452x338 μ m) were necessary to acquire the whole CA1 and CA3 regions, and five consecutive sections were analysed. Fluorojade B positive neurons were manually counted in both areas. Results are reported as the number of positive neurons per field of view and expressed as mean \pm SEM.

Quantification of the number of microglial cells

GFP positive cells were counted in confocal sections taken with 40x objective (size of the field of view 230x230 μ m). Similar laser intensity were used to acquire pictures of PBS- and kainate-injected animals. Cells were counted in 3 to 11 slices from each animal and 3 to 7 animals were analyzed for each condition. The number of cells counted in different slices of each animal was quite homogeneous and followed a Gaussian distribution. For each condition, we calculated the weighted average and its relative standard error to the mean (SEM). Anova with post-hoc Tukey test was applied to test significance between different groups.

RNA extraction and RT-PCR

Hippocampi from PBS- or kainate-injected mice were collected, frozen in liquid-nitrogen and stored at -80°C until RNA extractions were performed. Total RNA were extracted using the Trizol reagent (Invitrogen, Paisley, UK), then genomic DNA was digested using RNase-free DNase set (Qiagen) according to the manufacturer's protocols. Total RNA (2 μ g) was reverse transcribed into cDNA with random hexamers in a 20 μ l reaction by using a SuperScript III reverse transcriptase kit (Invitrogen, Paisley, UK). Quantitative real-time PCR (qRT-PCR) was performed in duplicate using four to six independent RNA samples. The cDNA was quantified using the Quantitect SYBR Green PCR kit and the Quantitect Primer assay kit (Qiagen) according to the manufacturer's instructions. The PCR amplification was run on 10 μ l of cDNA generated from 40 ng of total RNA and using an ABI PRISM 7900HT Sequence Detection System (Applied biosystems). For each reaction we calculated the difference (Δ Ct) between the cycle threshold (Ct) of the gene of interest and that of the housekeeping gene hypoxanthine-guanine phosphoribosyltransferase (HPRT). To quantify the fold changes in expression of each gene in kainate-injected animals compared to control, we first calculated the mean of Δ Ct obtained in four PBS injected animals (Δ Ct_{mPBS}). Then, for each kainate-injected animal, we calculated the ratio between ($2^{-\Delta$ Ct}) and ($2^{-\Delta$ Ct_{mPBS}}), i.e. $2^{-(\Delta$ Ct-

ΔC_{tm}^{PBS}) which estimates the fold change in expression of a given gene relative to the control animals (Livak and Schmittgen, 2001). Results are presented as the mean \pm SEM. Statistical significance compared to control was calculated using Student's t-test with Welch's correction, since standard deviations are usually different, and was established at * $p < 0.05$ and ** $p < 0.01$.

In vivo electrophysiological recordings

Mice were anesthetized with ketamine (100mg/Kg) and xylazine (5 mg/kg) and placed into a stereotaxic frame. Skulls surface was exposed and five electrodes were placed as following: Four extradural electrodes were inserted bilaterally in the parietal areas and one screwed at the level of the frontal area (ground electrode). Electrodes were plugged in a micro-connector with acrylic cement. After surgery, mice were allowed to recover for one week before recording. Freely moving animals were placed into individual Plexiglass boxes in a Faraday cage and their microconnectors plugged to an electroencephalographic (EEG) pre-amplifier box (Reega mini8, Alvar, Montreuil, France). The electrical activity recorded by derivation between extradural electrodes was filtered (pass-band 0.5-60 Hz) and acquired with a computer-based system (Micromed, Saint Etienne des Ouilères, France).

In vitro electrophysiological recordings

Hippocampal slices were obtained from 30-40 day old mice. Animals were killed by cervical dislocation, the brain was then quickly removed and placed in ice-cold artificial cerebrospinal fluid (aCSF) bubbled with carbogène (95% CO₂/5% O₂) and in which NaCl was replaced with sucrose (in mM: 210 sucrose, 2.5 KCl, 26 NaHCO₃, 1.25 NaH₂PO₄, 25 glucose, 1 CaCl₂, 7 MgSO₄; pH 7.4, osmolarity ~310 mOsm). Transverse 350 μ m thick slices were cut using a vibratome, transferred to a heated (34°C) holding chamber containing oxygenated (95% CO₂/5% O₂) standard aCSF (in mM: 124 NaCl, 3 KCl, 26 NaHCO₃, 1.25 NaH₂PO₄, 10 glucose, 2 CaCl₂, 1 MgCl) for 1h, and then subsequently maintained at room temperature.

Individual slices were transferred to a recording chamber on the stage of an Olympus microscope (BX50WI) with a 40x water immersion, equipped with cell-R imaging station including MT20 illumination system (Olympus, France) and a CCD camera (Hamamatsu ORCA2-AG, Massy, France). Slices were constantly perfused at room temperature (21-24°C) with oxygenated aCSF (3 ml/min). Unless otherwise stated, all drugs were applied through the general perfusion. Visually-identified GFP-expressing microglial cells were patched in whole-cell configuration in the *stratum radiatum* of the CA1 region of hippocampus.

Micropipettes (5 to 7 M Ω) were filled with a solution containing (in mM): K-gluconate 132, HEPES 11, EGTA 0.1, MgCl 4 (pH 7.35 adjusted with KOH, osmolarity ~300 mOsm), or Cs-gluconate 125, HEPES 10, EGTA 0.2, MgCl 1 (pH 7.35 adjusted with CsOH, osmolarity ~300 mOsm). Voltage-clamp recordings were performed using an Axopatch 200B (Axon Instrument, Union City, CA). Currents were low-pass filtered at 1-5 kHz, collected using PClamp 9 (Axon Instrument, Union City, CA) at a frequency 2-10 kHz and analyzed off line. An electrophysiological characterization in voltage-clamp was made at the beginning of the recording. Hyperpolarizing and depolarizing steps (from -140 to +40 mV for 50 ms) were used to determine I/V relationship of each recorded cell. Membrane input resistance and capacitance of the cells were determined from the current responses to voltage pulses ranging from -20mV to +20 mV from a holding potential of -60mV.

The responses induced by the activation of purinergic receptors were studied by bath applying ATP or selective agonists. In preliminary experiments, we observed that the responses to a second application, even performed after a delay of 15 to 20 minutes, could be different from the first one. This was particularly obvious for responses mediated by the activation of P2Y receptors studied with whole-cell recordings during which a wash-out of the evoked potassium currents occurred after about 10 minutes of dialysis. Changes in amplitude or kinetics were sometimes also observed for P2X receptor-mediated currents. Bath applications of agonists were therefore tested only once per slice. Consequently, all comparisons were done by testing differences between mean responses obtained from 1 microglia per slice, 3 to 4 slices per animal and 3 to 6 animals per experimental groups. The I/V curve of the responses induced by the activation of purinergic receptors were determined by subtracting the current responses to the same voltage step protocol applied in control conditions from those obtained in the presence of the agonists.

Data were analyzed off-line using Clampfit (Axon Instrument, Union City, CA). Data values are presented as mean \pm SEM. Statistical significance was tested with the program GraphPAD InStat. First we tested if data were sampled from populations that follow Gaussian distributions using the method Kolmogorov and Smirnov. Then according to the result, non-parametric test (Mann-Whitney) or parametric test that assumes the standard deviation can be different (t-test with Welch's correction) were used to compare results between the two groups of data. Statistical significance was established at * $p < 0.05$ and ** $p < 0.01$.

Imaging experiments

Slices were placed in the recording chamber at 34°C and after 5 minutes (taken as t_0) a pipette containing 2-MeSADP (100 μ M) was placed in the *stratum radiatum* in the center of the field of view. Movement of microglia processes were followed by taking a fluorescent image every minute through a 40X water immersion objective (Olympus, NA 0.8). To quantify the elongation of the GFP positive processes toward the pipette we measured the fluorescence in two concentric circles, one close to the pipette ($F_{c_{int}}$, blue circle in fig 8) and a second covering almost the whole field of view ($F_{c_{ext}}$, light blue circle in fig 8). We then calculated the ratio of the fluorescence in the two circles at different time points (t) and subtracted the ratio at t_0

$$F_{c_{int}}(t)/F_{c_{ext}}(t) - F_{c_{int}}(t_0)/F_{c_{ext}}(t_0),$$

The obtained values were then normalized to the maximum.

To estimate the velocity at which the fluorescent processes elongated toward the pipette, a series of concentric circles were drawn as region of interest and the fluorescence was measured in concentric rings (F_r). Since the microglia processes approach the pipette with approximately a circular symmetry, it was possible to observe for each ring a maximum in the temporal course of the fluorescence. F_r was normalized to the fluorescence of the external circle, and the following ratio was calculated for each ring

$$F_r(t)/F_{c_{ext}}(t) - F_r(t_0)/F_{c_{ext}}(t_0)$$

and then normalized to its maximum.

To define the velocity, the distance between two coronal sections was divided by the time difference between the corresponding two peaks of fluorescence. We considered only the experiments where we could clearly identify at least three peaks of fluorescence in three coronal sections, thus two velocities, and the mean was taken as the representative velocity of each experiment. Data are given as mean \pm SEM, and a Student's t-test with Welch's correction was used to compare results between control and kainate injected mice. Statistical significance was established at * $p < 0.05$ and ** $p < 0.01$.

Reagents

Tetrodotoxin (TTX), D-(-)-2-Amino-5-phosphonopentanoic acid (D-AP5), 2,3-Dioxo-6-nitro-1,2,3,4-tetrahydrobenzo[f]quinoxaline-7-sulfonamide (NBQX), gabazine, kainate, Pyridoxalphosphate-6-azophenyl-2',5'-disulfonic acid (iso-PPADS), 4-Aminopyridine, LY 341495; 8-cyclopentyl-1-3-dipropylxanthine (DPCPX) were purchased from Tocris Bioscience (Bristol, UK) or Ascent Scientific (Weston-Super-Mare, UK); 2-

(Methylthio)adenosine-5'-(trihydrogen diphosphate) (2-MeSADP), Brilliant Blue G (BBG), ATP, UDP, ivermectine, from Sigma-Aldrich (Lyon, France).

In experiments involving BBG, slices were incubated in a solution containing BBG (3 μ M) for 30 min at 37°C 3 μ M and then kept at room temperature until the experiment.

Results

Characterization of kainate-induced status epilepticus model in C57BL/6 CX3CR1^{eGFP/+} mice

To study microglia activation during the early phases of epilepsy, we used i.p. injections of kainate as a non-invasive model of status epilepticus (SE). In rats, systemic injection of kainate has been considered as valuable model of temporal lobe epilepsy (Ben Ari and Cossart, 2000). However, models of experimental epilepsy are less well characterized in mice and the susceptibility to seizures varies dramatically across mouse strains (Schauwecker, 2002). Therefore, we first characterized the inflammatory reaction and the extent of neuronal damage in the hippocampus of the CX3CR1^{eGFP/+} mice following a status epilepticus.

Eighty percent of the kainate-injected mice survived of which 70 % developed a status epilepticus corresponding to stages 4 or 5 on the Racine scale (see methods) and were used for subsequent analysis. Quantitative PCR experiments performed on hippocampi from 4 control mice and 4-6 kainate-injected mice revealed a 10 to 22 fold increase in the expression of the mRNAs coding for the pro-inflammatory molecules IL-1 β , IL-6, TNF- α and COX-2 (fig 1A) 3 hours after SE. At 24 hours post SE, the expression of TNF- α was further increased (80.7 +/- 9.2 fold) compared to 3 hours (19.7 +/- 5 fold) while that of COX2 was decreased (5.7 +/- 1.6 versus 22.6 +/- 1.9 at 3 hours), but remained higher than in control animals. At 48 hours post SE, the increase in expression of the 4 genes was more variable and remained significant only for TNF- α and COX-2. These results confirmed the occurrence of an inflammatory reaction during the 48 hours that follow a SE and which is comparable to that observed in other experimental models of epilepsy (Vezzani and Granata, 2005).

We then examined neuronal damage in the hippocampus of CX3CR1^{eGFP/+} mice at 24 and 48 hours post SE with eosin-hematoxylin staining. Following SE, there was a time-dependent increase of the number of black and large neuronal morphologies observed in the cell layers of the hippocampus. Neuronal degeneration was first observed in CA3 24h after SE (data not shown) and extended to the CA1 area 48h after SE (Fig 1B). Similar observations were made using the specific degenerating marker FluoroJade B (Schmued and Hopkins, 2000). While no staining was observed in control mice, many neurons were labeled at 24h (data not shown) and 48h after the induction of SE. The number of cells per field of view (442 x 338 μ m) counted 48h post SE was 31.5 ± 2.7 and 18 ± 2.42 in CA1 and CA3 regions, respectively. These observations are in good agreement with a previous study reporting neuronal damage in the hippocampus of C57BL/6 mice after kainate-induced seizures (Benkovic et al., 2004), even though neuronal degeneration in these mice is clearly less massive than in other mouse

strains as previously shown (McKhann et al., 2003). Furthermore, *in vivo* EEG recordings performed 48h post SE (n=4 animals) but also 50 days post SE (n=2 animals) revealed the occurrence of bilateral synchronized bursting activities (Fig. 1D) which were not observed in control mice (n=4 animals).

Altogether, these data indicate that kainate-induced seizures in CX3CR1^{eGFP/+} mice lead to an inflammatory reaction associated with neuronal death in the hippocampus and trigger long term changes of electrical brain activity. Because neuronal damage appeared more pronounced in CA1, we focused our investigation of microglia activation in this region of the hippocampus.

Activation of Microglia after kainate-induced SE

As previously reported for the CX3CR1^{eGFP/+} mouse line (Cardona et al., 2006), GFP co-localized with the specific marker of microglia Iba1 (fig 2A), but not with the neuronal marker NeuN, the astrocytic marker GFAP nor with NG2, a marker of oligodendrocyte precursors (data not shown). We then investigated changes in microglia morphology and immuno-reactivity in the hippocampus 3, 24 and 48 hours after the induction of the SE. A higher Iba1 immuno-reactivity was first observed by immuno-fluorescence in the hippocampus of treated animals 24h after the kainate injection (fig. 2A). At this stage microglia had larger soma and thicker primary processes when compared with control animals (fig 2A). We never observed, however, GFP positive cells with amoeboid macrophage-like morphology. At 48h post SE, similar changes of morphology and Iba1 immuno-reactivity were observed and the increased expression of Iba1 was confirmed by a Western blot analysis performed on hippocampal extracts (Fig 2B; 3 control and 3 epileptic mice).

This increased expression of Iba1 proteins in the hippocampus of epileptic mice could be in part explained by a change in the number of microglia. We thus evaluated whether there were a proliferation of microglial cells in kainate injected mice. At 24 and 48h after the induction of SE there was a significant increase (ANOVA test, $p < 0.001$) in the number of microglial cells in CA1 (fig 2C). The number of cells per field of view (230 x 230 μm) rose from 16.96 ± 0.54 in control to 25.31 ± 0.61 after 24h and to 31.80 ± 0.54 after 48h. Post-hoc Tukey test revealed significant difference ($p < 0.001$) between all groups. This proliferation of microglia was similar in the dorsal and ventral hippocampus (data not shown). Consistent with the increase number of microglia, immuno-stainings for the proliferation marker ki67 and for MAC2, a specific marker of activated microglia in proliferation (Lalancette-Hebert et al.,

2007) were observed in microglial cells in the CA1 area 24h after the kainate injection and became more evident at 48h (fig 3).

Thus, status epilepticus evoked by systemic injection of kainate in CX3CR1^{eGFP/+} mice triggers an activation of hippocampal microglia characterized by a change in morphology and a cell proliferation.

Intrinsic membrane properties of activated and non-activated microglia

There has been a limited number of studies on the electrophysiological properties of microglia *in situ* but work in cultures showed that changes of intrinsic membrane properties occurs during microglia activation (Farber and Kettenmann, 2005). We thus used whole-cell recordings in acute hippocampal slices of control and epileptic CX3CR1^{eGFP/+} mice to characterize electrophysiological properties of microglial cells identified by the expression of GFP. Because the slicing procedure might result in activating microglia, in particular near the surface of the slice, recordings were obtained from cells usually at a depth below 30 μm from the slice surface. In addition, experiments were completed within the first 4 hours after slicing.

Resting microglial cells in slices of control mice had a high membrane input resistance of $3.6 \pm 0.2 \text{ G}\Omega$ and a membrane capacitance of $28.1 \pm 1.0 \text{ pF}$ ($n=37$, Fig. 4A). Application of hyperpolarizing and depolarizing voltage steps from a holding potential of -60 mV did not induce large voltage dependant membrane currents (Fig. 4B) and the membrane I/V relationship was almost linear (Fig. 4C). Microglial cells recorded 3h after SE had similar intrinsic membrane properties ($n=7$, Fig. 4B & C) while at 24h post SE microglia had a larger membrane capacitance ($32.9 \pm 1.8 \text{ pF}$; $p=0.018$, $n=15$) when compared to control mice but a similar input resistance ($3.0 \pm 0.3 \text{ G}\Omega$; $p=0.17$). In addition, voltage activated currents were evoked when applying hyperpolarizing and depolarizing pulses (Fig. 4B), leading to rectifications in the I/V curve (Fig. 4C). Forty eight hours after SE, microglia cells had larger membrane capacitance (35.6 ± 1.6 , $p<0.001$; $n=42$) and lower input resistance ($2.2 \pm 0.1 \text{ G}$, $p<0.001$) compared to control mice. Moreover, inward currents evoked by hyperpolarizing pulses were smaller while outward currents evoked by depolarizing pulses were larger than at 24h post SE (fig. 4C). As illustrated in figure 4C, the difference in amplitude described for voltage activated currents remained significant when normalizing the current values to the cell capacitance to take into account the difference in cell size between non-activated and activated microglia. Both inward and outward currents were absent when microglia was

recorded with an intracellular solution containing the non-selective potassium channel blocker Cesium, while outward currents were abolished by 4-aminopyridine (1 mM, n=4, data not shown), a blocker of outward rectifying potassium channels. These results indicate that intrinsic membrane properties of microglia gradually evolve during the first two days that follow a SE.

Increased expression of purinergic receptor mRNAs in the hippocampus after status epilepticus

Activation of purinergic receptors plays an essential role in different processes of microglia activation (Sperlagh et al., 2006;Farber et al., 2008). We therefore tested whether their expression was changed after SE. Quantitative PCR was performed on whole hippocampi from control animals and 3, 24, 48 hours after the induction of status epilepticus to compare the mRNA expression of ionotropic P2X1, P2X4 and P2X7 and of metabotropic P2Y6, P2Y12 and P2Y13 purinergic receptors. This specific set of receptors has been selected on the basis of previous studies that have established their expression in microglia or macrophages ((Inoue et al., 2007). Already 3h after SE there was a small but significant increase (1.60 ± 0.05 fold) in the expression of P2Y6 mRNAs whereas that of P2X4 and P2Y13 mRNAs decreased and that of P2X1, P2X7, P2Y12 and P2Y13 mRNAs did not change significantly (Fig. 5). The pattern of expression of these receptors 24h after status epilepticus was characterized by an important increase of P2Y6 mRNAs expression (9.2 ± 1.5 fold). Forty eight hours after SE, the expression of all 4 receptors was above control values with a 7.5 ± 1.2 fold increase for P2Y6, a 3.5 ± 0.2 fold increase for P2Y12, a 3.4 ± 0.2 fold increase for P2X1, a 2.0 ± 0.2 fold increase for P2Y13, a 2.0 ± 0.2 fold increase for P2X4 and a 1.9 ± 0.2 fold increase for P2X7 receptor mRNAs.

These results suggest that all purinergic receptors known to be expressed in microglia are up-regulated in the hippocampus 48h after SE. In the case of P2Y12 receptors, our results contrast markedly with the down-regulation of this receptor in some other models of microglia activation (Moller et al., 2000;Haynes et al., 2006). Because the qPCR analysis was performed on total RNA from whole hippocampi and not on isolated microglia, we verified by immuno-cytochemistry that the expression this receptor was indeed restricted to microglia and was not down-regulated in the hippocampus 48h after SE (supplementary fig.1).

Enhanced purinergic responses of activated microglia after status epilepticus

We then tested whether the enhanced expression of purinergic receptor mRNAs in the whole hippocampus after SE correlated with changes in responses of microglia to purinergic receptor activation. A preliminary series of experiments in control animals showed that hippocampal microglia cells respond to bath applied ATP (1mM for 2 min) with a complex response composed of inward and outward currents probably mediated by P2X and P2Y receptors, respectively. These responses were not altered by blocking synaptic transmission (n=5) with TTX (1 μ M), NBQX (10 μ M), APV (50 μ M) and gabazine (5 μ M), while they were greatly reduced by the large spectrum antagonist of purinergic receptors PPADS (100 μ M; n=3, data not shown). New series of experiments were therefore designed to analyze the effect of status epilepticus on isolated P2X and P2Y receptor-mediated components of these responses.

Responses mediated by the activation of P2X receptors were isolated by recording microglia with an intracellular solution containing Cesium to block potassium currents induced by P2Y receptor activation (Fig. 6A). Inward currents evoked by ATP (1mM for 2 min) at a holding potential of -40 mV had an average amplitude of 4.8 ± 0.6 pA (n=12) in microglia of control mice. These currents had an I/V curve which presented a slight inward rectification with a reversal potential near 0 mV, as expected for non selective cation permeable channels (Fig. 6A). The amplitude and the I/V curve of these responses (n=4) were not altered in the presence of a cocktail aimed at reducing indirect effects through neuronal activation and including TTX (1 μ M), NBQX (10 μ M), APV (50 μ M) and gabazine (5 μ M) (supplementary figure 2). Removing extracellular divalent ions greatly increased the amplitude of the ATP-induced currents (49.3 ± 7.6 pA at -40 mV, n=6) without changing the form of the I/V curve (Fig. 6B & 6C). The antagonist of P2X7 receptors, Brilliant Blue G (BBG, 3 μ M) blocked a large part of the ATP currents (residual current at -40 mV: 1.6 ± 0.3 , n=3) and the further addition of the antagonist of ionotropic purinergic receptors isoPPADS (50 μ M) did not antagonize more the responses (Fig. 6C). The sensitivity of the responses to extracellular divalent cations and to BBG suggests that P2X7 receptors were responsible for most of the response induced by ATP in non-activated microglia.

The responses due to the activation of ionotropic purinergic receptors in activated microglia were then analyzed 48h after SE when the enhanced expression of the corresponding mRNAs was most pronounced (see above and Fig. 5). The amplitude of the currents induced in standard extracellular medium by ATP was larger in activated microglia than in control mice (13.2 ± 1.9 pA, n= 14; p<0.01). As illustrated in figure 6A and 5C, this difference remained

significant when normalizing the current values to the cell capacitance to take into account the difference in cell size between non-activated and activated microglia. As shown in figure 6C, the responses were greatly reduced by BBG (3 μ M) but in contrast to the responses of non-activated microglia, the residual current (3.9 ± 0.4 pA at -40mV, n=5) was further decreased by adding isoPPADS (residual current: 1.7 ± 0.4 pA, n=4). As in non-activated microglia, removing divalent cations from the extracellular solution enhanced ATP responses of microglia from epileptic mice and these responses were larger (156.9 ± 23.0 pA; n=9; Fig 6B & 6C) compared to control animals ($p < 0.01$). BBG (3 μ M) decreased ATP responses in Mg-Ca-free solutions and the residual current (28.8 ± 6.8 pA, n=4) was further reduced by adding isoPPADS (5.8 ± 1.0 pA, n=3). These results indicate a higher expression of functional P2X7 receptors in activated microglia and suggest the presence of another type of P2X receptor responsible of the BBG resistant component of the response. It is worth noting that ATP responses recorded in our experimental conditions were not sensitive to the positive modulator of P2X4 receptors, ivermectin (5 μ M, data not shown), suggesting that these receptors did not mediated the BBG resistant component observed in activated microglia.

We then investigated the responses to P2Y receptor activation. Microglia cells were voltage clamped at -20mV with a K-gluconate based internal solution and the responses to bath applied selective agonists of P2Y receptors were tested. The P2Y6 agonist UDP (1 mM, 1 min) induced an outward current in all microglia recorded in hippocampal slices of both control and epileptic animals (Fig. 7A). However, the amplitude current induced in activated microglia was about six times larger in epileptic animals (7.1 ± 1.1 pA, n=9, and 44.3 ± 11 pA, n=8, in control and kainate injected animals, respectively; $p = 0.01$). As for P2X receptor mediated responses, this difference was not due to the larger size of activated microglial cells since it remained significant when the responses were expressed in current densities (Fig. 7).

Differences between control and epileptic mice were also observed with an agonist at both P2Y12 and P2Y13 receptors, 2-MeSADP (100 μ M, 1 minute): the currents induced in activated microglia (46.8 ± 13.8 pA, n=7) were significantly larger than those recorded in slices of control mice (6.5 ± 1.0 , n=11, $p < 0.05$). The amplitude of the currents induced by both agonists decreased with hyperpolarization and reached their zero value close to -90 mV, as expected for potassium currents (see I/V curves in Fig. 7A & 7B). In addition, the amplitude and the I/V of responses to UDP (n=4) and to 2-MeSADP (n=4) were not altered in the presence of TTX (1 μ M), NBQX (10 μ M), APV (50 μ M), gabazine (5 μ M), LY341495 (100 μ M) and DPCPX (1 μ M) (supplementary figure 2).

Thus, together with the results of quantitative PCR, these observations indicate the occurrence of an increase in expression of functional P2Y receptors receptors in activated microglia two days after a status epilepticus.

Activated microglial cells have higher motility in the hippocampus of epileptic mice

Microglia can readily send their processes towards an ATP source (Davalos et al., 2005; Haynes et al., 2006) that, in pathological conditions, would be generated by damaged cells or a prolonged hyper-activity. This phenomenon is partially mediated by P2Y₁₂ receptors (Haynes et al., 2006). We therefore compared the elongation velocity of the processes of GFP expressing microglia in acute hippocampal slices of control and epileptic mice. In time-laps video-microscopy experiments, we observed that processes of microglia elongated towards a pipette containing ATP (1 mM, data not shown) or 2-MeSADP (100 μM) in slices from both epileptic and control mice (see movies 1 and 2 in supplementary material). No directional movement was observed when the pipette contained extracellular solution without purinergic receptor agonist (data not shown). The velocity with which the processes reached the pipette was significantly faster in slices of epileptic animals compared to control (fig 8, A and B). To quantify these differences, we measured the temporal course of the ratio between the fluorescence in a circle around the pipette and that in a circle which covers almost the entire field of view. This ratio increased as the processes approach the pipette. The mean time to reach the maximum of this ratio was 54.7 ± 2.1 min in control animals (n=13) and 28.4 ± 2.8 min in epileptic mice (n=14; p<0.01).

There is a higher density of microglia in epileptic animals (see above Fig. 2C). Therefore, this difference could be due to the fact that more microglial cells are closer to the pipette containing purinergic agonist. We thus estimated the velocity by measuring the time differences at which peaks of fluorescence appeared in concentric rings along the elongation path toward the pipette (Fig. 8B and 8D, see methods for details). The estimated velocity in slices of control mice was 3.32 ± 0.24 μm/min (n=10) while that in kainate injected mice was 5.85 ± 0.6 μm/min (n=10, p<0.01). To evaluate a possible contribution of neuronal activity, experiments with 2-MeSADP were repeated in the presence of TTX (1 μM), NBQX (10 μM), APV (50 μM) and gabazine (5 μM). The velocity with which microglia processes elongated toward the pipette containing the agonist was 3.19 ± 0.12 μm/min (n=7) in control animals and increased to 4.97 ± 0.49 μm/min (n=4) in epileptic mice (p<0.01). These values were not significantly different from those measured in normal medium (p>0.4). These observations

indicate that increased velocity of microglia processes observed after SE was a consequence of changes in P2Y receptor signaling in microglial cells.

Discussion

In addition to the observed changes in morphology and in Iba1 expression, our study provides the first description of microglia functional changes during the inflammatory reaction that follows a status epilepticus. We show that this activation is characterized by a proliferation, a modification of intrinsic membrane properties, an increase of purinergic receptor-mediated responses and an enhanced process motility of microglia.

The model of status epilepticus in CX3CR1^{eGFP/+} C57BL/6 mice

There is an important variability in the susceptibility of different mouse strains, in response to systemic injections of kainate, to develop seizures and to display the characteristic pattern of hippocampal neurodegeneration observed in rats (Pisa et al., 1980; Sperk et al., 1983; Ben-Ari, 1985) and the strain C57BL/6 mice has been considered as one of the most resistant (Schauwecker and Steward, 1997; Schauwecker, 2002; McKhann et al., 2003; Mazarati et al., 2004; Shikhanov et al., 2005). However, recent evidence indicates that seizures and some degree of hippocampal neurodegeneration also occur in these mice (Benkovic et al., 2004; McLin and Steward, 2006; Benkovic et al., 2006). In agreement with these latter observations, we could trigger stage 4 to 5 seizures in CX3CR1^{eGFP/+} C57BL/6 mice and fluorajade B labeled a significant number of CA1 neurons after kainate-induced SE in these mice. This susceptibility was probably not a consequence of the use of mice heterozygotes for CX3CR1 since similar increases in the expression of inflammatory mediators were also observed in wild type C57BL/6 mice (data not shown). A previous study on the role of CX3CR1 receptors showed that the functions of microglia in various experimental models of brain disorders are impaired in CX3CR1^{eGFP/eGFP} but not in CX3CR1^{eGFP/+} mice (Cardona et al., 2006). Together with the rapid and prolonged increase expression of pro-inflammatory molecules and the activation of microglia, our results thus validate the use of intra-peritoneal injection of kainate in these mice as a model of status epilepticus. Whether this status epilepticus leads to the development of chronic epilepsy remains to be established but our data suggest that kainate-treated mice have abnormal hippocampal hyper-excitability up to 2 months after the induction of SE.

Intrinsic membrane properties of microglia

Until recently, the difficulty to identify microglia has precluded the analysis of their functional state *in situ* and most of our current knowledge on electrophysiological properties of microglia and their changes during activation relies on studies performed in culture systems. There are few exceptions though and, similarly to what we observed in hippocampal slices of control mice, other studies reported that non-activated microglia in acute brain slices has almost linear I/V curves with virtually no voltage activated channels (Boucsein et al., 2000;Wu et al., 2007). Yet, cultured microglia expresses a prominent inward rectifying current at hyperpolarizing potentials in absence of any specific activation stimulus (Farber and Kettenmann, 2005). Boucsein et al (Boucsein et al., 2000) also observed in slices of the facial nucleus after lesion of the facial nerve that in activated microglia an inward rectifying current is first expressed, followed by the expression of additional outward currents. Our present study provides further support for this sequential activation of different voltage activated channels during the development of inflammation *in situ*, with the inward rectifying current being maximum first (i.e. at 24h post SE) and a delayed expression of the outward current. Furthermore, we observed a decrease in amplitude of the inward rectifying current at 48h post SE when the outward current reaches its maximum amplitude. This pattern of activation resembles that observed in cultured microglia in which application of the pro-inflammatory toxin lipopolysaccharide (LPS) induces the expression of outward currents together with the decrease in amplitude of the already present inward rectifying current (Boucsein et al., 2000). Thus, changes in intrinsic membrane properties during the activation of microglia follow the same sequence of events in the three experimental conditions where they have been studied (i.e. in cultures, *in vivo* after axotomy and after status epilepticus). Therefore, in contrast with some other aspects of microglia activation (see below and (Hanisch and Kettenmann, 2007) for review), up-regulation of potassium channels does not seem to be differentially regulated according to the context of the activation. It is worth noting, however, that the up-regulation of different potassium channels may be a prerequisite for triggering different subsequent aspects of microglia activation (Fordyce et al., 2005;Pannasch et al., 2006;Franciosi et al., 2006;Kaushal et al., 2007).

Enhanced purinergic responses in activated microglia

Microglial cells express both metabotropic (P2Y) and ionotropic (P2X) purinergic receptors. Accordingly and in agreement with previous studies (Boucsein et al., 2003;Wu et al., 2007), we found that ATP application evoked complex responses composed of inward and outward currents. By investigating separately P2X and P2Y receptor mediated responses, we found

that both ionotropic and metabotropic components of purinergic responses were enhanced in activated microglia following SE. This enhancement of purinergic responses probably involves an increased expression of the corresponding receptor since P2X and P2Y mRNAs were up-regulated in the epileptic hippocampus. Our study provides electrophysiological evidence that activation of microglia *in situ* involves an increase of all types of purinergic responses.

Pharmacological investigations point toward a major role of P2X7 receptors in the ATP response mediated by ionotropic receptors which were increased in divalent cation free solution and strongly reduced by BBG. Though, an iso-PPADS sensitive but BBG resistant component was found in activated microglia, suggesting that the enhanced purinergic response would be partially mediated also by another type of P2X receptors, among which P2X1 is a possible candidate. However, the rapid desensitization and the poor selectivity of pharmacological tools available for ionotropic purinergic receptors makes their study difficult in slices and imposes caution in the interpretation of results about the role of specific receptor subtype. In models of LPS-induced inflammation, P2X7 receptors support the release of IL-1beta by microglia (Ferrari et al., 1997; Rampe et al., 2004; Choi et al., 2007; Mingam et al., 2008) but they probably also regulate indirectly the expression or release of other inflammatory factors such as cyclooxygenase-2, IL-6, IL-12 and TNFalpha (Rampe et al., 2004; Choi et al., 2007). P2X7 receptors, probably in association with Pannexin-1 (Pelegrin and Surprenant, 2006) could therefore play a central role in the secretion of inflammatory mediators which occurs during the 48 hours that follow SE as these receptors could also control the microglia proliferation (Bianco et al., 2006). Finally, the observation that P2X7 (and other P2 receptors see below) expression is significantly enhanced after the induction of the SE while the cytokine expression is also enhanced suggests the occurrence of a positive feedback mechanism exacerbating the activation process.

The most dramatic difference we observed between non-activated and activated microglia is the up-regulation of P2Y6 receptors. The mRNA expression already increased 3 hours after SE and reaches a plateau between 24 and 48 hours when electrophysiological responses to UDP are 6 times larger than in non-activated microglia. This increased expression of P2Y6 receptors has been observed in other models of microglia activation *in vitro* but also *in vivo* (Bianco et al., 2005; Koizumi et al., 2007). Accordingly, this receptor sustains a key function of microglia since its activation is essential in triggering phagocytosis (Koizumi et al., 2007). Thus, enhanced UDP mediated currents observed in the present study would mediate the enhanced phagocytic action observed in microglia of epileptic animals (Koizumi et al., 2007).

Non-activated microglia constantly move their processes to probe their environment (Davalos et al., 2005; Nimmerjahn et al., 2005). Following a local lesion, microglia cells send their process toward the lesion and ATP has been proposed to be one of the “alarm signals” since a source of exogenous ATP (or ATP analogue) mimics this phenomenon *in vivo* (Davalos et al., 2005; Haynes et al., 2006) as well as in slices (Wu et al., 2007). P2Y12 receptors mediate this chemotaxis (Haynes et al., 2006) and the potassium currents induced by the activation of P2Y12 receptor seem also to be essential (Wu et al., 2007). Our results show that activated microglial cells respond to a P2Y12-13 receptor agonist (2-MeSADP) with larger outward potassium currents and, as a functional consequence, the velocity with which their processes reach a source of 2-MeSADP is twice faster than for non-activated microglia. Despite the lack of evidence for the involvement of P2Y13 receptors in microglia chemotaxis and the fact that up-regulation of P2Y12 receptor mRNAs is twice larger than that of P2Y13 receptors in the epileptic hippocampus, we cannot totally rule out the possibility that P2Y13 receptors contribute to the increase in velocity of microglia processes after SE. It worth noting, however, that P2Y13 transcripts but not receptor proteins were detected in brain microglia (Moller et al., 2000; Haynes et al., 2006). Thus, increase in both P2Y6 and P2Y12 receptor-mediated responses confers to activated microglia the ability to intervene faster onto damaged cells since they would have larger responses to both the “eat-me” and “find me” signals.

A specific activation state of microglia after status epilepticus

The analysis of purinergic responses reveals striking differences between models of microglia activation. In contrast to the up-regulation of P2X7 receptors that we observed, a down regulation of P2X7 receptors has been reported in cultured microglia stimulated with LPS (Bianco et al., 2005), suggesting that regulation of P2X7 receptors is dependent on the stimulus or on the context in which activation is induced. Along the same line, we observed that P2Y12 mRNAs are up-regulated and P2Y12 receptor-mediated responses are increased in activated microglia of the epileptic hippocampus. This is in agreement with the increased expression of P2Y12 receptor observed in spinal chord microglia in a model of neuropathic pain (Kobayashi et al., 2008) but contrasts markedly with the down regulation of this receptor in models of neuronal injury *in vitro*, of LPS injection *in vivo* and *in vitro* (Moller et al., 2000; Haynes et al., 2006). In these latter models, the down-regulation of P2Y12 receptors correlates with the progression of microglia morphology toward an amoeboid state (Haynes et al., 2006). Interestingly, microglial cells in the hippocampus after SE, which clearly maintains their expression of P2Y12 receptors (see supplementary fig. 1), undergo morphological

changes but never progress toward a full amoeboid morphology. Thus, the absence of amoeboid microglia together with the up-regulation of P2X7 and P2Y12 receptors indicate that microglia in the epileptic hippocampus is in a specific activation state which differs from that occurring during stronger inflammatory reactions triggered by severe neuronal injury or by LPS. This state, characterized by a maintained ability to release cytokines (P2X7) and by an enhanced chemotaxis (P2Y12), might be correlated with the persistent hyper-excitability of the hippocampal neuronal networks which outlasts the duration of the status epilepticus *per se*. Whether microglia acquires a similar functional state in other brain disorders associated with chronic and probably milder inflammation remains to be studied.

Reference List

- Ben Ari Y, Cossart R (2000) Kainate, a double agent that generates seizures: two decades of progress. *Trends Neurosci* 23:580-587.
- Ben-Ari Y (1985) Limbic seizure and brain damage produced by kainic acid: mechanisms and relevance to human temporal lobe epilepsy. *Neuroscience* 14:375-403.
- Benkovic SA, O'Callaghan JP, Miller DB (2004) Sensitive indicators of injury reveal hippocampal damage in C57BL/6J mice treated with kainic acid in the absence of tonic-clonic seizures. *Brain Res* 1024:59-76.
- Benkovic SA, O'Callaghan JP, Miller DB (2006) Regional neuropathology following kainic acid intoxication in adult and aged C57BL/6J mice. *Brain Res* 1070:215-231.
- Bianco F, Ceruti S, Colombo A, Fumagalli M, Ferrari D, Pizzirani C, Matteoli M, Di Virgilio F, Abbracchio MP, Verderio C (2006) A role for P2X7 in microglial proliferation. *J Neurochem* 99:745-758.
- Bianco F, Fumagalli M, Pravettoni E, D'Ambrosi N, Volonte C, Matteoli M, Abbracchio MP, Verderio C (2005) Pathophysiological roles of extracellular nucleotides in glial cells: differential expression of purinergic receptors in resting and activated microglia. *Brain Res Brain Res Rev* 48:144-156.
- Boucsein C, Kettenmann H, Nolte C (2000) Electrophysiological properties of microglial cells in normal and pathologic rat brain slices. *Eur J Neurosci* 12:2049-2058.
- Boucsein C, Zacharias R, Farber K, Pavlovic S, Hanisch UK, Kettenmann H (2003) Purinergic receptors on microglial cells: functional expression in acute brain slices and modulation of microglial activation in vitro. *Eur J Neurosci* 17:2267-2276.
- Cardona AE, Piroo EP, Sasse ME, Kostenko V, Cardona SM, Dijkstra IM, Huang D, Kidd G, Dombrowski S, Dutta R, Lee JC, Cook DN, Jung S, Lira SA, Littman DR, Ransohoff RM (2006) Control of microglial neurotoxicity by the fractalkine receptor. *Nat Neurosci*.
- Chessell IP, Hatcher JP, Bountra C, Michel AD, Hughes JP, Green P, Egerton J, Murfin M, Richardson J, Peck WL, Grahames CB, Casula MA, Yiangou Y, Birch R, Anand P, Buell GN (2005) Disruption of the P2X7 purinoceptor gene abolishes chronic inflammatory and neuropathic pain. *Pain* 114:386-396.
- Choi HB, Ryu JK, Kim SU, McLarnon JG (2007) Modulation of the purinergic P2X7 receptor attenuates lipopolysaccharide-mediated microglial activation and neuronal damage in inflamed brain. *J Neurosci* 27:4957-4968.
- Choi J, Koh S (2008) Role of brain inflammation in epileptogenesis. *Yonsei Med J* 49:1-18.
- Coull JA, Beggs S, Boudreau D, Boivin D, Tsuda M, Inoue K, Gravel C, Salter MW, De Koninck Y (2005) BDNF from microglia causes the shift in neuronal anion gradient underlying neuropathic pain. *Nature* 438:1017-1021.

Crespel A, Coubes P, Rousset MC, Brana C, Rougier A, Rondouin G, Bockaert J, Baldy-Moulinier M, Lerner-Natoli M (2002) Inflammatory reactions in human medial temporal lobe epilepsy with hippocampal sclerosis. pp 159-169.

Davalos D, Grutzendler J, Yang G, Kim JV, Zuo Y, Jung S, Littman DR, Dustin ML, Gan WB (2005) ATP mediates rapid microglial response to local brain injury in vivo. *Nat Neurosci* 8:752-758.

De Simoni MG, Perego C, Ravizza T, Moneta D, Conti M, Marchesi F, De Luigi A, Garattini S, Vezzani A (2000) Inflammatory cytokines and related genes are induced in the rat hippocampus by limbic status epilepticus. *Eur J Neurosci* 12:2623-2633.

Eriksson C, Van Dam AM, Lucassen PJ, Bol JG, Winblad B, Schultzberg M (1999) Immunohistochemical localization of interleukin-1beta, interleukin-1 receptor antagonist and interleukin-1beta converting enzyme/caspase-1 in the rat brain after peripheral administration of kainic acid. *Neuroscience* 93:915-930.

Farber K, Kettenmann H (2005) Physiology of microglial cells. *Brain Res Brain Res Rev* 48:133-143.

Farber K, Markworth S, Pannasch U, Nolte C, Prinz V, Kronenberg G, Gertz K, Endres M, Bechmann I, Enjyoji K, Robson SC, Kettenmann H (2008) The ectonucleotidase cd39/ENTPDase1 modulates purinergic-mediated microglial migration. *Glia* 56:331-341.

Ferrari D, Chiozzi P, Falzoni S, Dal SM, Melchiorri L, Baricordi OR, Di VF (1997) Extracellular ATP triggers IL-1 beta release by activating the purinergic P2Z receptor of human macrophages. *J Immunol* 159:1451-1458.

Fordyce CB, Jagasia R, Zhu X, Schlichter LC (2005) Microglia Kv1.3 channels contribute to their ability to kill neurons. *J Neurosci* 25:7139-7149.

Franciosi S, Ryu JK, Choi HB, Radov L, Kim SU, McLarnon JG (2006) Broad-spectrum effects of 4-aminopyridine to modulate amyloid beta1-42-induced cell signaling and functional responses in human microglia. *J Neurosci* 26:11652-11664.

Franke H, Gunther A, Grosche J, Schmidt R, Rossner S, Reinhardt R, Faber-Zuschratter H, Schneider D, Illes P (2004) P2X7 receptor expression after ischemia in the cerebral cortex of rats. *J Neuropathol Exp Neurol* 63:686-699.

Hanisch UK, Kettenmann H (2007) Microglia: active sensor and versatile effector cells in the normal and pathologic brain. *Nat Neurosci* 10:1387-1394.

Haynes SE, Hollopeter G, Yang G, Kurpius D, Dailey ME, Gan WB, Julius D (2006) The P2Y12 receptor regulates microglial activation by extracellular nucleotides. *Nat Neurosci* 9:1512-1519.

Inoue K, Koizumi S, Tsuda M (2007) The role of nucleotides in the neuron--glia communication responsible for the brain functions. *J Neurochem* 102:1447-1458.

Jung S, Aliberti J, Graemmel P, Sunshine MJ, Kreutzberg GW, Sher A, Littman DR (2000) Analysis of fractalkine receptor CX(3)CR1 function by targeted deletion and green fluorescent protein reporter gene insertion. *Mol Cell Biol* 20:4106-4114.

- Kaushal V, Koeberle PD, Wang Y, Schlichter LC (2007) The Ca²⁺-activated K⁺ channel KCNN4/KCa_{3.1} contributes to microglia activation and nitric oxide-dependent neurodegeneration. *J Neurosci* 27:234-244.
- Kobayashi K, Yamanaka H, Fukuoka T, Dai Y, Obata K, Noguchi K (2008) P2Y₁₂ receptor upregulation in activated microglia is a gateway of p38 signaling and neuropathic pain. *J Neurosci* 28:2892-2902.
- Koizumi S, Shigemoto-Mogami Y, Nasu-Tada K, Shinozaki Y, Ohsawa K, Tsuda M, Joshi BV, Jacobson KA, Kohsaka S, Inoue K (2007) UDP acting at P2Y₆ receptors is a mediator of microglial phagocytosis. *Nature* 446:1091-1095.
- Lalancette-Hebert M, Gowing G, Simard A, Weng YC, Kriz J (2007) Selective ablation of proliferating microglial cells exacerbates ischemic injury in the brain. *J Neurosci* 27:2596-2605.
- Livak KJ, Schmittgen TD (2001) Analysis of relative gene expression data using real-time quantitative PCR and the 2^{-ΔΔC_T} Method. *Methods* 25:402-408.
- Mazarati A, Lu X, Shinmei S, Badie-Mahdavi H, Bartfai T (2004) Patterns of seizures, hippocampal injury and neurogenesis in three models of status epilepticus in galanin receptor type 1 (GalR1) knockout mice. *Neuroscience* 128:431-441.
- McKhann GM, Wenzel HJ, Robbins CA, Sosunov AA, Schwartzkroin PA (2003) Mouse strain differences in kainic acid sensitivity, seizure behavior, mortality, and hippocampal pathology. *Neuroscience* 122:551-561.
- McLin JP, Steward O (2006) Comparison of seizure phenotype and neurodegeneration induced by systemic kainic acid in inbred, outbred, and hybrid mouse strains. *Eur J Neurosci* 24:2191-2202.
- Mingam R, De S, V, Amedee T, Bluthe RM, Kelley KW, Dantzer R, Laye S (2008) In vitro and in vivo evidence for a role of the P2X₇ receptor in the release of IL-1 beta in the murine brain. *Brain Behav Immun* 22:234-244.
- Moller T, Kann O, Verkhratsky A, Kettenmann H (2000) Activation of mouse microglial cells affects P2 receptor signaling. *Brain Res* 853:49-59.
- Nimmerjahn A, Kirchhoff F, Helmchen F (2005) Resting microglial cells are highly dynamic surveillants of brain parenchyma in vivo. *Science* 308:1314-1318.
- Ohsawa K, Irino Y, Nakamura Y, Akazawa C, Inoue K, Kohsaka S (2007) Involvement of P2X₄ and P2Y₁₂ receptors in ATP-induced microglial chemotaxis. *Glia* 55:604-616.
- Pannasch U, Farber K, Nolte C, Blonski M, Yan CS, Messing A, Kettenmann H (2006) The potassium channels Kv1.5 and Kv1.3 modulate distinct functions of microglia. *Mol Cell Neurosci* 33:401-411.
- Pelegrin P, Surprenant A (2006) Pannexin-1 mediates large pore formation and interleukin-1beta release by the ATP-gated P2X₇ receptor. *EMBO J* 25:5071-5082.

Pisa M, Sanberg PR, Corcoran ME, Fibiger HC (1980) Spontaneously recurrent seizures after intracerebral injections of kainic acid in rat: a possible model of human temporal lobe epilepsy. *Brain Res* 200:481-487.

Rampe D, Wang L, Ringheim GE (2004) P2X7 receptor modulation of beta-amyloid- and LPS-induced cytokine secretion from human macrophages and microglia. *J Neuroimmunol* 147:56-61.

Rock RB, Peterson PK (2006) Microglia as a pharmacological target in infectious and inflammatory diseases of the brain. *J Neuroimmune Pharmacol* 1:117-126.

Schauwecker PE (2002) Complications associated with genetic background effects in models of experimental epilepsy. *Prog Brain Res* 135:139-148.

Schauwecker PE, Steward O (1997) Genetic determinants of susceptibility to excitotoxic cell death: implications for gene targeting approaches. *Proc Natl Acad Sci U S A* 94:4103-4108.

Schmued LC, Hopkins KJ (2000) Fluoro-Jade B: a high affinity fluorescent marker for the localization of neuronal degeneration. *Brain Res* 874:123-130.

Sheng JG, Boop FA, Mrak RE, Griffin WS (1994) Increased neuronal beta-amyloid precursor protein expression in human temporal lobe epilepsy: association with interleukin-1 alpha immunoreactivity. *J Neurochem* 63:1872-1879.

Shikhanov NP, Ivanov NM, Khovryakov AV, Kaspersen K, McCann GM, Kruglyakov PP, Sosunov AA (2005) Studies of damage to hippocampal neurons in inbred mouse lines in models of epilepsy using kainic acid and pilocarpine. *Neurosci Behav Physiol* 35:623-628.

Skaper SD, Facci L, Culbert AA, Evans NA, Chessell I, Davis JB, Richardson JC (2006) P2X(7) receptors on microglial cells mediate injury to cortical neurons in vitro. *Glia*.

Sperk G, Lassmann H, Baran H, Kish SJ, Seitelberger F, Hornykiewicz O (1983) Kainic acid induced seizures: neurochemical and histopathological changes. *Neuroscience* 10:1301-1315.

Sperlagh B, Vizi ES, Wirkner K, Illes P (2006) P2X7 receptors in the nervous system. *Prog Neurobiol* 78:327-346.

Tsuda M, Shigemoto-Mogami Y, Koizumi S, Mizokoshi A, Kohsaka S, Salter MW, Inoue K (2003) P2X4 receptors induced in spinal microglia gate tactile allodynia after nerve injury. *Nature* 424:778-783.

Vesce S, Rossi D, Brambilla L, Volterra A (2007) Glutamate release from astrocytes in physiological conditions and in neurodegenerative disorders characterized by neuroinflammation. *Int Rev Neurobiol* 82:57-71.

Vezzani A, Granata T (2005) Brain inflammation in epilepsy: experimental and clinical evidence. *Epilepsia* 46:1724-1743.

Vezzani A, Ravizza T, Balosso S, Aronica E (2008) Glia as a source of cytokines: implications for neuronal excitability and survival. *Epilepsia* 49 Suppl 2:24-32.

Viviani B, Gardoni F, Marinovich M (2007) Cytokines and neuronal ion channels in health and disease. *Int Rev Neurobiol* 82:247-263.

Wu LJ, Vadakkan KI, Zhuo M (2007) ATP-induced chemotaxis of microglial processes requires P2Y receptor-activated initiation of outward potassium currents. *Glia* 55:810-821.

Wyss-Coray T, Mucke L (2002) Inflammation in neurodegenerative disease--a double-edged sword. *Neuron* 35:419-432.

Figure Legends:

Figure 1. Status epilepticus induced by intraperitoneal kainate injection triggers inflammation, neuronal death in the hippocampus and long term changes in EEG activity in CXCR1^{eGFP/+} mice. **A**, Changes in expression of pro-inflammatory markers in the hippocampus analyzed by qPCR at different time points after induction of the status epilepticus. Ten to 20 fold increase in mRNA expression for IL-1 β , IL-6, TNF- α and COX-2 changes were observed at 3h (n=4 mice) compared to control (PBS; n=4). Significant increased expression persisted at 24h (n=6) for all mRNA species and became more variable at 48 hours (n=6). **B**, Fluorochrome B (left panels) and Eosine-hematoxylin staining (right panels) in the CA1 area of the ventral hippocampus in PBS (top panels) and kainate-injected mice (bottom panels) 48h after the status epilepticus. Note the strong staining of the pyramidal cell layer with both techniques in kainate injected mice. Scale bar 200 μ m. **C**, Representative cortical EEG-recording from a mouse 2 months after induction of status epilepticus. The representative trace exhibits spontaneous collective activity in a form burst of spikes discharges. The burst is showed at higher temporal resolution in the inset, where individual spike discharge can be identified.

Figure 2. Increase in size and number of microglia in the hippocampus after status epilepticus. **A**. Confocal images (stack of 21 z sections, 8.28 μ m total thickness) of Iba1 immunostaining and GFP fluorescence in the CA1 stratum radiatum of CX3CR1^{eGFP/+} mice in control conditions (top panels) and 24h after induction of the status epilepticus (bottom panels). The two markers are co-localised, confirming that GFP expressing cells are microglia. Note the stronger Iba1 immunoreactivity, the larger somata and the thicker proximal processes of activated microglia. Scale bar 15 μ m. **B**, Western blot analysis of Iba1 expression in the hippocampus of control and kainate-injected animals after 24 and 48h. Samples were obtained from hippocampi of 3 animals for each condition. **C**, Quantification of microglial cell number in fields of view of 230x230 μ m in the CA1 area of control (n=4) and treated mice 24h (n=3) and 48h (n=7) after the induction of the status epilepticus. The number of microglial cells was significantly larger already at 24h and had doubled at 48h. ** p< 0.01

Figure 3. Microglia proliferates after status epilepticus. Confocal images of GFP fluorescence and of immunostaining of the proliferation markers Ki67 (left series of panels, scale bar 25 μ m) and Mac-2 (right series of panels, scale bar 40 μ m). Representative pictures (stack of 5 z

sections, 4.5 μm total thickness) of the CA1 hippocampal region obtained from PBS injected mice and from mice sacrificed 3, 24, and 48h after the induction of status epilepticus. Immunostaining for both markers, highly co-localized with GFP, is first observed at 24h and increases at 48h.

Figure 4. Time dependent changes in intrinsic electrophysiological properties of microglia after status epilepticus. **A**, Temporal course of input resistance (left panel) and membrane capacitance (right panel) changes of CA1 hippocampal microglial cells after status epilepticus. * $p < 0.05$, ** $p < 0.01$. **B**, Examples of current responses induced by voltage steps of 20 mV increment from -140 to +60mV (holding potential -60mV) in microglia cells of control (left panel, black traces) and KA injected animals 48h after status epilepticus (right panel, gray traces). **C**, I/V curves obtained from microglial cells recorded from control mice (black squares, $n=35$) and from mice 3 h (open circles, $n=7$), 24h (half filled circles, $n=15$) and 48h (filled circles, $n=39$). Current densities were considered to take into account changes in membrane capacitance in activated microglia. Note the appearance of inward rectifying currents at hyperpolarized potentials and of outward currents at depolarized potentials 24h after the status epilepticus. Note also that the inward rectifying currents decrease while the outward currents increase at 48h. There was no significant difference between the I/V curves of control and 3h conditions.

Figure 5. Status epilepticus induces an increase of purinergic receptor mRNA expression in the hippocampus. **A**) Quantitative PCR of purinergic receptors in whole hippocampi from control animals ($n=4$) and from treated animals at 3h ($n=4$), 24h ($n=6$) and 48h ($n=6$) after the status epilepticus. Note that the expression of P2Y6 was already increased at 3h while that of other receptors was increased at 24h or 48h.

Figure 6. Larger P2X receptor-mediated responses in activated microglia. **A**, **B**, Examples of currents induced by bath application of ATP (black bars, 1mM, 2 minutes) in microglia from control animals (left panel, black traces) and from mice 48h after a status epilepticus (right panel, gray traces) in normal (**A**) and Mg^{2+} - Ca^{2+} -free medium (**B**). Cells were patched with a Cs-gluconate based internal solution and hold at -40mV. The vertical fast deflexions correspond to currents generated by voltage step series applied to obtain the I/V curves of the ATP responses shown on the right. Graphs on the right represent the average of ATP induced current density/voltage relation in control (black squares, $n=12$ for control medium and $n=6$

for Ca^{2+} - Mg^{2+} -free medium) and 48h after status epilepticus (gray circles, n=13 for control medium and n=9 for Ca^{2+} - Mg^{2+} -free medium) obtained by subtracting I/V curve obtained before from that obtained during ATP application. **C**, Pharmacology of the P2X receptor-mediated responses induced by ATP (1 mM) application at -40mV in control (black bars) and 48h after status epilepticus induction (gray bars). Responses were enhanced in Mg^{2+} - Ca^{2+} -free medium and strongly reduced by Brilliant Blue G (BBG, 3 μM) in control as in activated microglia. However, a residual current which was blocked by further addition of isoPPADS (50 μM) was present in activated microglia. * p<0.05, ** p< 0.01.

Figure 7. Larger P2Y6 and P2Y12 receptor-mediated responses in activated microglia. **A**, Examples of currents induced by bath application of the P2Y6 receptor agonist UDP (black bars, 1mM, 1 minute) in microglia from a control animal (left panel, black trace) and from a mice 48h after the status epilepticus (right panel, gray trace). Cells were patched with K-gluconate based solution and responses were tested at -20mV. **B**, I/V curve of the UDP induced responses in control (black symbols, n=9) and epileptic mice (gray symbols, n=8). **C**, Same as in (**B**) for the P2Y12 receptor mediated responses induced by the selective agonist 2-MeSADP application (100 μM , 1 minute). Numbers of microglia are 11 in control (black bar/symbols) and 7 in treated mice (gray bar/symbols). * p<0.05.

Figure 8. Higher motility of microglia processes after a status epilepticus. **A**, Examples of fluorescence images at different time point after the insertion (at t=0, first column) in the slice of a pipette containing 2-MeSADP (100 μM) in control (upper row) and 48h after the induction of a status epilepticus (bottom panels). The pictures at t=15 min (second column) show the formation of a ring of fluorescence corresponding to microglia processes elongated from cells at the periphery of the field of view towards the pipette tip in the center. At t=25 min (right column) the processes of activated microglia have reached the pipette (lower picture) while those of microglia from control mice have not yet completed their extension (upper picture). Scale bar: 50 μm . **B**, Normalised ratio of the internal over the external circle fluorescence (top, left panel; see methods) in experiments on control (black, n=5 slices) and epileptic (red, n=6 slices) mice 48h after status epilepticus. This ratio increases when the fibres approach the pipette and reaches its maximum when all the processes are within the central circle. **C**, Temporal evolution of the total fluorescence measured in concentric rings (orange second, red third, blue 4th, green 5th, order starting from the external light blue ring). Left and right panels correspond to the example in control (top panels in **A**) and 48h after

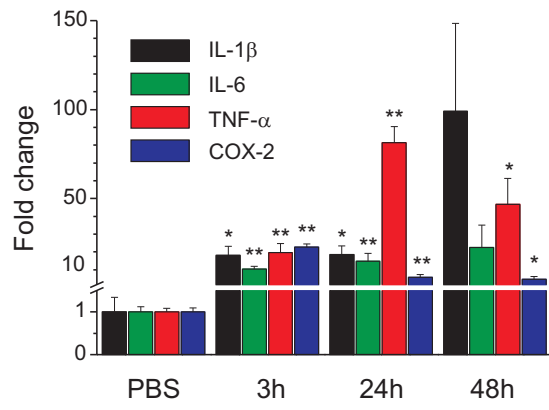
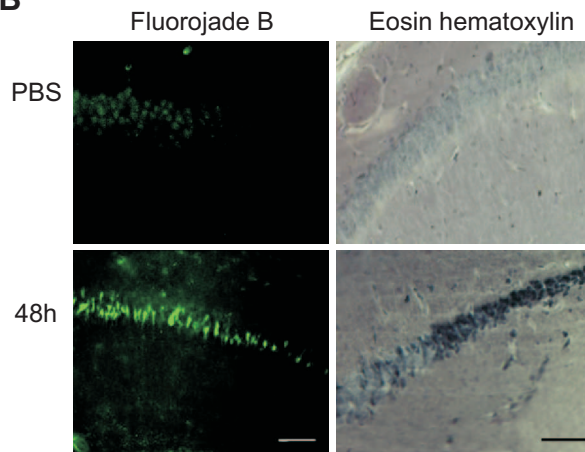
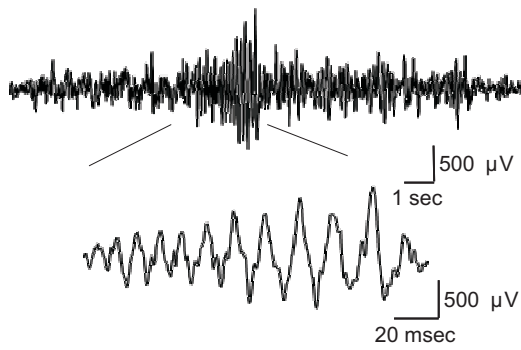
status epilepticus induction (bottom panels in **A**), respectively. The distance between peaks provides a measure of the velocity of the processes. Averages of the velocity measured in slices of control (black, n=7) and epileptic (red, n=4) mice are represented on the histogram in inset. ** p< 0.01.

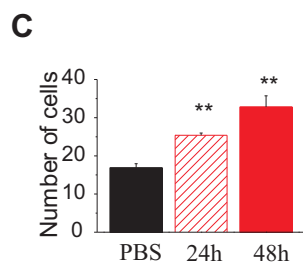
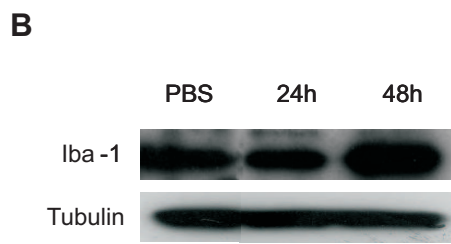
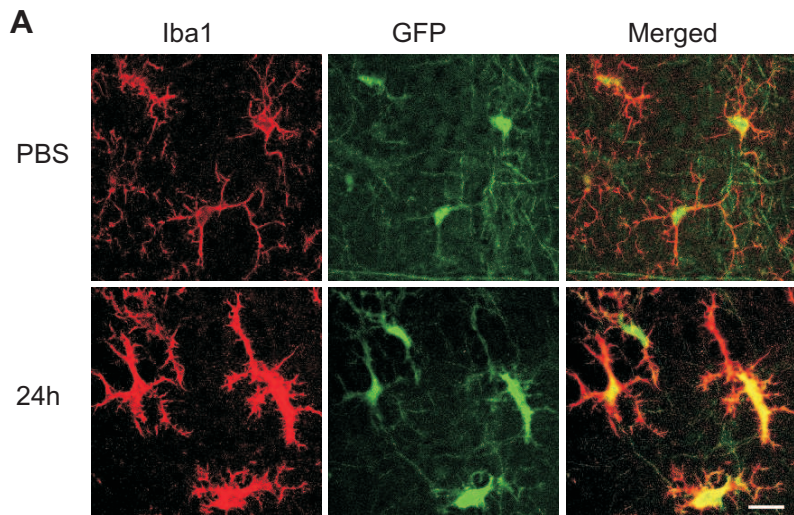
Supplemental figure 1. Activated microglia cells still express P2Y12 receptors. Confocal images (stack of 13 z sections, 11.7 μm total thickness) of eGFP fluorescence and P2Y12 immunostaining in the CA1 stratum radium of CX3CR1^{eGFP/+} mice in control conditions (top panels) and 48h after induction of the status epilepticus (bottom panels). The two markers are co-localized, confirming that P2Y12 is expressed only in microglia. Scale bar 20 μm .

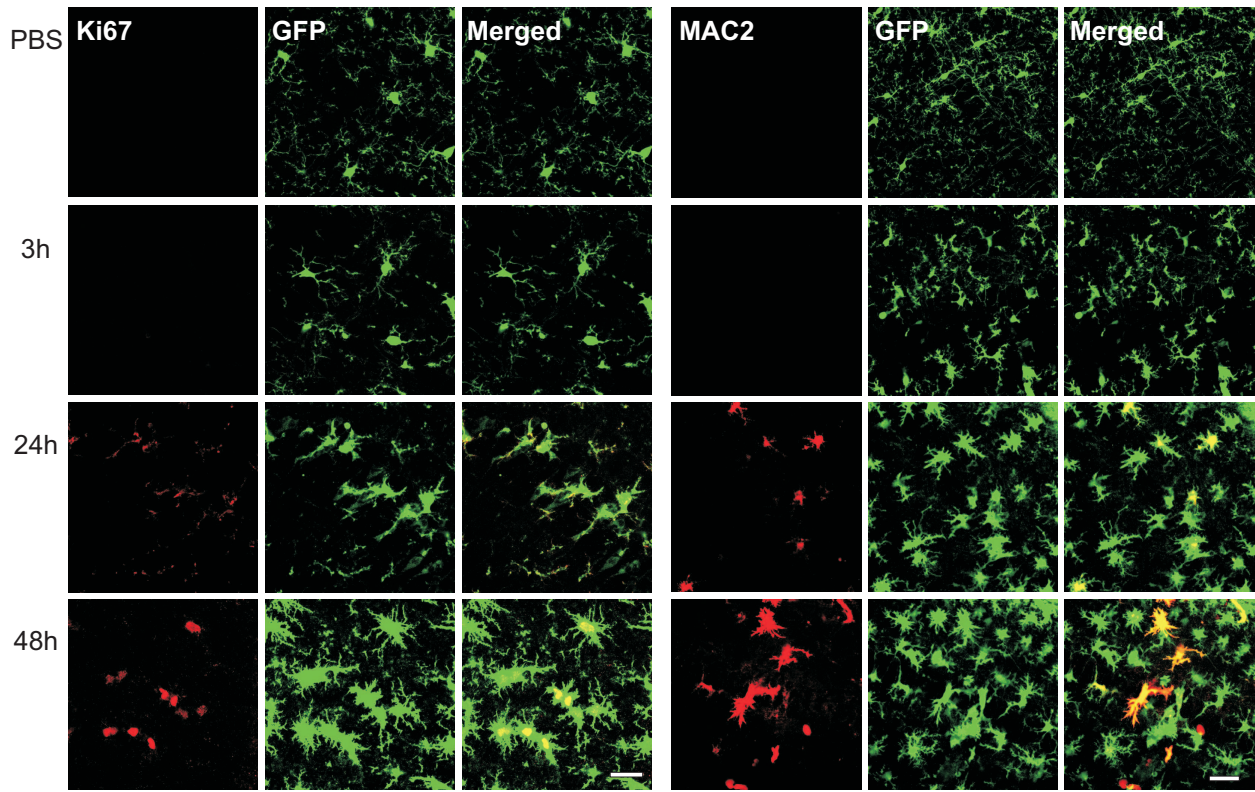
Supplemental figure 2. Purinergic responses in microglia are not affected by reducing synaptic transmission. Examples of currents induced in microglia of control animals by bath application of ATP (**A**, 1mM for 2 minutes), UDP (**B**, 1mM for 1minute) and 2-MeSADP (**C**, 100 μM for 1minute) in the presence of TTX (1 μM), NBQX (20 μM), gabazine (10 μM), D-AP5 (20 μM). In panels **B** and **C**, LY341495 (100 μM), DPCPX (1 μM) were also added. The histograms show the comparison of the agonist-induced currents in control experiments (black bars, same data as those of figures 6 and 7) and in experiments done in presence of the cocktails of antagonists (hatched bars, n=4 for each case). Reduction of neuronal and synaptic activities did not change the mean amplitudes of the currents induced by purinergic receptor agonists.

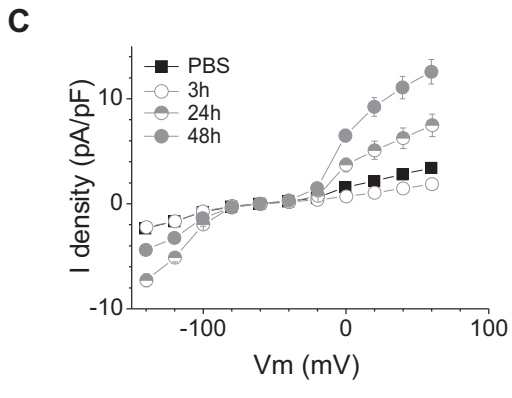
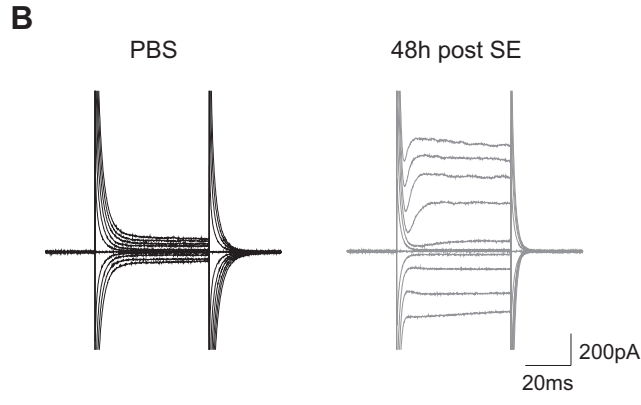
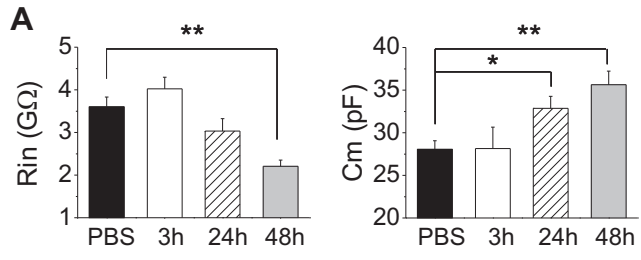
Supplemental Video 1. Motility of microglial cell processes towards a point source of P2Y12 receptor agonist. This movie shows the dynamics of microglial cell processes after the insertion of a pipette containing 2-MeSADP (100 μM) in an acute hippocampal slice of a PBS injected animal. After the insertion of the pipette, the microglial processes extend towards the pipette tip (red spot) and reach it in about 1 hour. Images were taken once every minute.

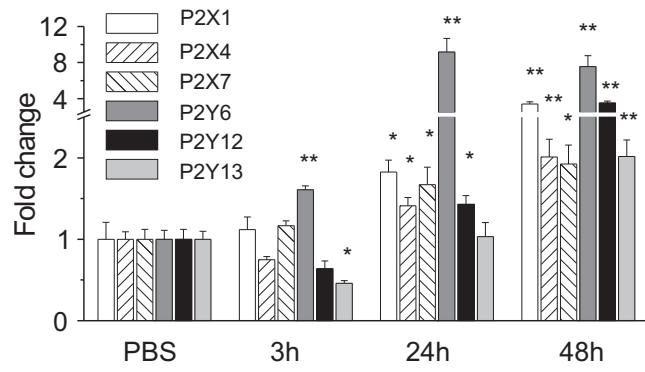
Supplemental Video 2. Increased motility of microglial cell processes after a status epilepticus. Same experimental conditions as in supplemental video 1 on a hippocampal slice of kainate-injected animal 48 hours after status epilepticus. The extension of the processes towards the pipette tip (red spot) containing 2-MeSADP (100 μM) was faster than in control animals and was completed in less than 30 minutes. Images were taken once every minute.

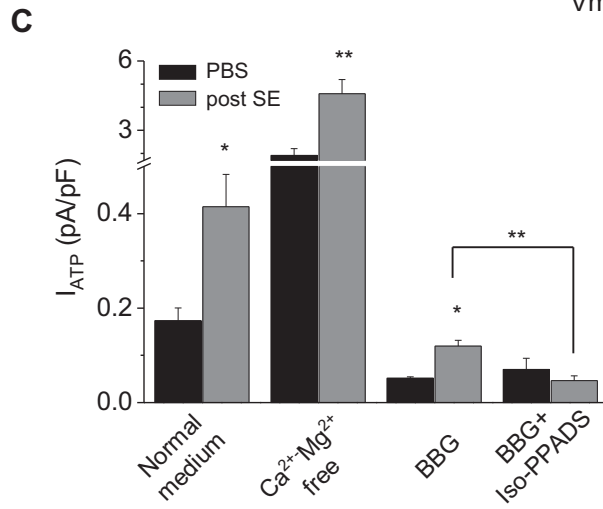
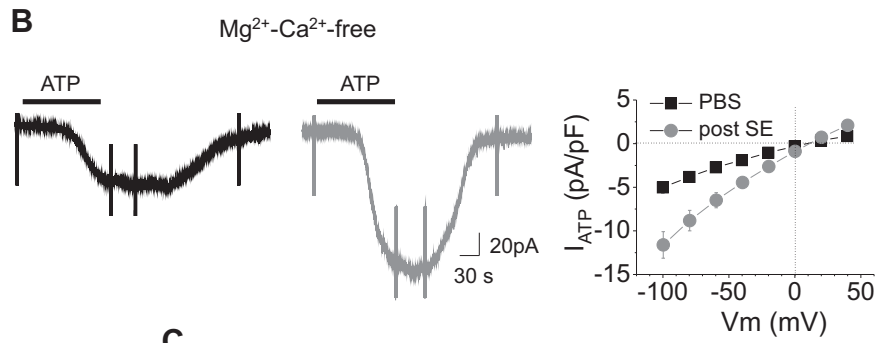
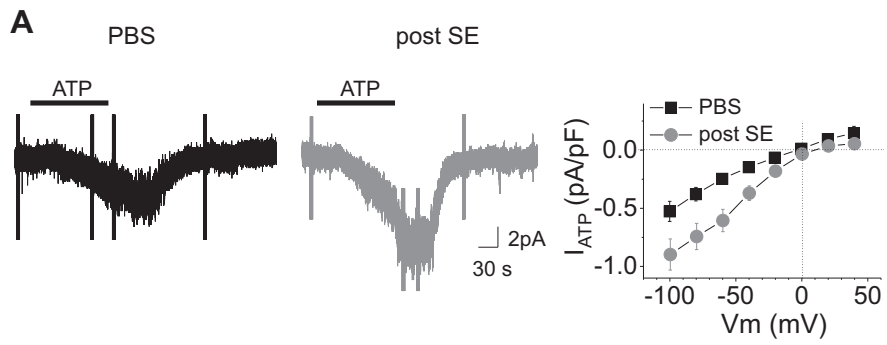
A**B****C**

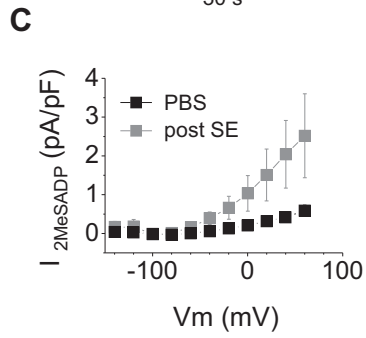
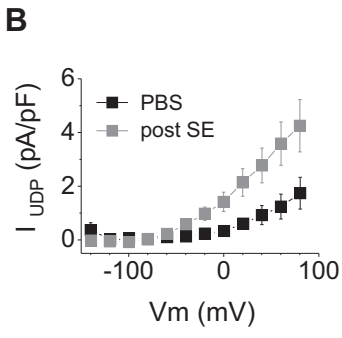
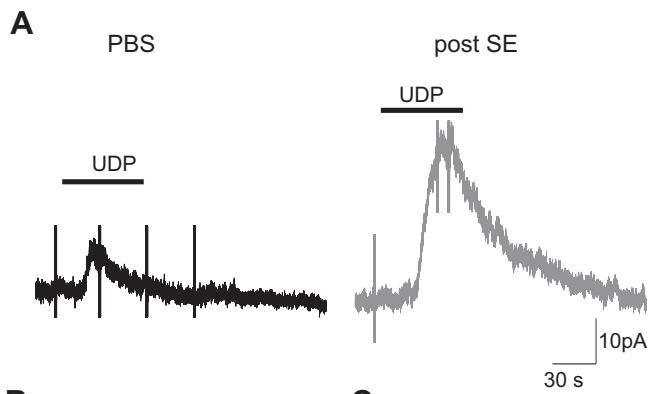


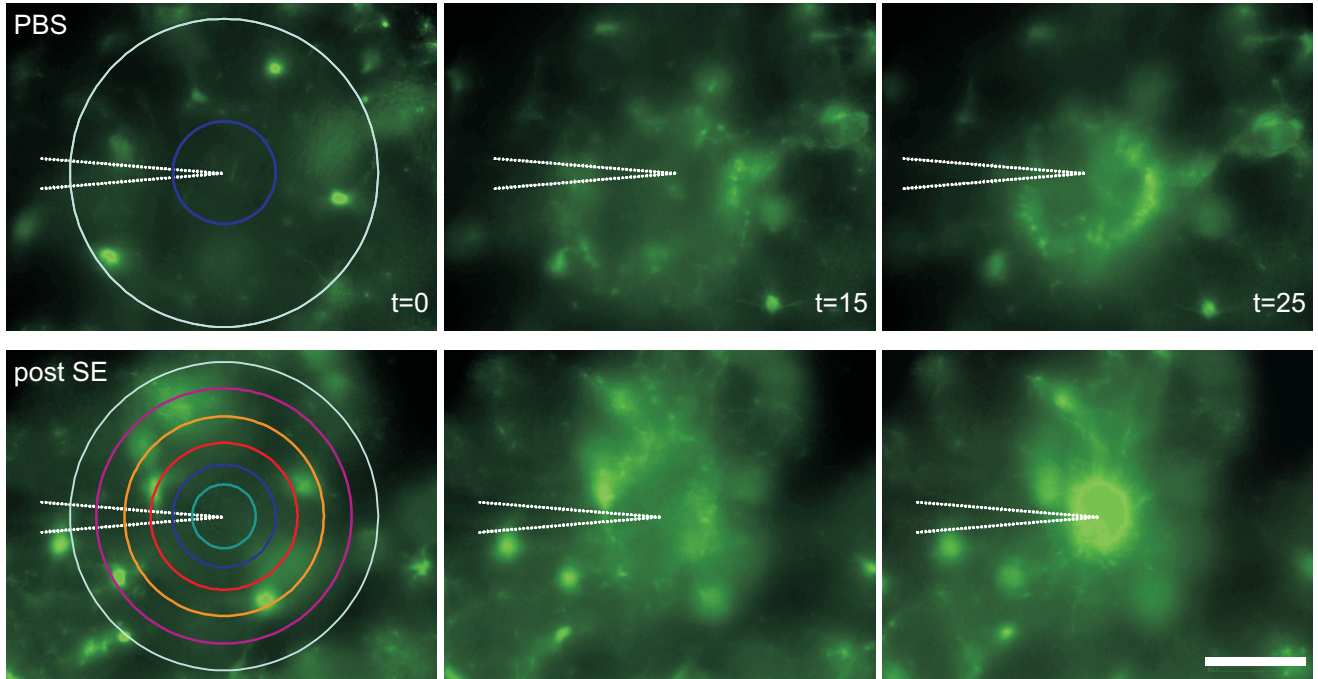
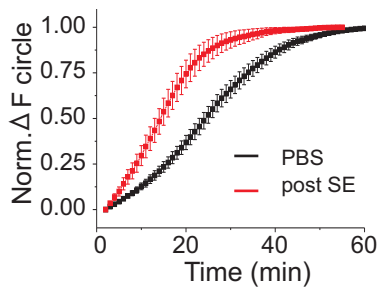










A**B****C**